vaccines

MDPI

Article

Interferon-α-Induced Dendritic Cells Generated with Human Platelet Lysate Exhibit Elevated Antigen Presenting Ability to Cytotoxic T Lymphocytes

Ippei Date [1], Terutsugu Koya [1,2], Takuya Sakamoto [1,2], Misa Togi [1,2], Haruhiko Kawaguchi [1], Asuka Watanabe [1], Tomohisa Kato, Jr. [3] and Shigetaka Shimodaira [1,2,*]

[1] Department of Regenerative Medicine, Kanazawa Medical University, Uchinada, Kahoku 920-0293, Japan; dat-pey@kanazawa-med.ac.jp (I.D.); koya@kanazawa-med.ac.jp (T.K.); taku0731@kanazawa-med.ac.jp (T.S.); m-togi@kanazawa-med.ac.jp (M.T.); harukawa@kanazawa-med.ac.jp (H.K.); asuka-w@kanazawa-med.ac.jp (A.W.)

[2] Center for Regenerative Medicine, Kanazawa Medical University Hospital, Uchinada, Kahoku 920-0293, Japan

[3] Medical Research Institute, Kanazawa Medical University, Uchinada, Kahoku 920-0293, Japan; tkato@kanazawa-med.ac.jp

* Correspondence: shimodai@kanazawa-med.ac.jp; Tel.: +81-76-218-8304

Abstract: Given the recent advancements of immune checkpoint inhibitors, there is considerable interest in cancer immunotherapy provided through dendritic cell (DC)-based vaccination. Although many studies have been conducted to determine the potency of DC vaccines against cancer, the clinical outcomes are not yet optimal, and further improvement is necessary. In this study, we evaluated the potential ability of human platelet lysate (HPL) to produce interferon-α-induced DCs (IFN-DCs). In the presence of HPL, IFN-DCs (HPL-IFN-DCs) displayed high viability, yield, and purity. Furthermore, HPL-IFN-DCs displayed increased CD14, CD56, and CCR7 expressions compared with IFN-DCs produced without HPL; HPL-IFN-DCs induced an extremely higher number of antigen-specific cytotoxic T lymphocytes (CTLs) than IFN-DCs, which was evaluated with a human leukocyte antigen (HLA)-restricted melanoma antigen recognized by T cells 1 (MART-1) peptide. Additionally, the endocytic and proteolytic activities of HPL-IFN-DCs were increased. Cytokine production of interleukin (IL)-6, IL-10, and tumor necrosis factor (TNF)-α was also elevated in HPL-IFN-DCs, which may account for the enhanced CTL, endocytic, and proteolytic activities. Our findings suggest that ex-vivo-generated HPL-IFN-DCs are a novel monocyte-derived type of DC with high endocytic and proteolytic activities, thus highlighting a unique strategy for DC-based immunotherapies.

Keywords: immunotherapy; dendritic cells; vaccine; human platelet lysate; tumor-associated antigens; cytotoxic T lymphocyte; endocytosis; proteolytic activity

1. Introduction

Dendritic cells (DCs) are antigen-presenting cells (APCs) that play a central role in immune acquisition [1]. DCs are widely expressed on body surfaces and in tissues characterized by distinct phenotypes, origins, receptors, and functions [2]. Human DCs in the blood can be divided into conventional DCs (cDCs) and plasmacytoid DCs (pDCs). cDCs are involved in the stimulation of CD4+ and CD8+ T cells whereas pDCs produce type 1 interferon (IFN) in response to a virus [3]. Recently, single-cell RNA sequencing has been used to genetically classify human blood DCs into six new subtypes [4]. Conversely, Langerhans cells and dermal DCs are found in human skin. Dermal DCs are classified into CD14+ DCs, CD141+ DCs, and CD1c+ DCs, which have been investigated for their functional relationship, similar to blood DCs [5]. Furthermore, DCs play a role in anti-cancer immunity and the prevention of infectious agents. Of the DC subsets, blood CD141+

DCs have a high antigenic cross-presentation capability, and thus, contribute to anti-tumor immunity [6]. Apart from distinct DC subsets in vivo, there are monocyte-derived DCs that can be produced ex vivo [7]. DCs take up tumor-associated antigens released from tumor cells and migrate to the lymph nodes, where they present these peptides to naïve CD8^{+} T cells through the human leukocyte antigen (HLA). CD8^{+} T cells primed by DCs become cytotoxic T lymphocytes (CTLs), which are recruited to the tumor microenvironment to kill tumor cells [8].

Since the 1990s, monocyte-derived DCs loaded with tumor-specific peptides such as Wilms tumor 1 (WT1) have been utilized in clinical studies and trials as vaccines against a variety of cancers [9]. In recent years, clinical trials have been conducted that combine these DCs with chemotherapy, such as S-1, and immune checkpoint inhibitors, such as nivolumab and ipilimumab [10–12]. Moreover, there has been significant interest in clinical studies on personalized vaccines, which use DC vaccines with autologous whole tumor lysates to amplify T cells that target somatic mutation-derived neoantigens [13].

Per the standardized manufacturing protocol of DC vaccines, leukapheresis is performed on cancer patients to collect monocyte-rich peripheral blood at the first step. Then, adherent cells isolated from the peripheral blood are stimulated with granulocyte macrophage colony-stimulating factor (GM-CSF) and interleukin (IL)-4 to differentiate into immature DCs. Various methods can be used to induce the maturation of these immature DCs, including the addition of cytokines such as tumor necrosis factor (TNF)-α; adjuvants such as lipopolysaccharide (LPS), a component of the outer membrane of the cell wall of gram-negative bacteria; and a cocktail of the streptococcal preparations OK-432 and prostaglandin E_2 (PGE$_2$) [14,15]. DC vaccines manufactured via these methods are administered intradermally to the axilla and/or groin, and DCs that take up tumor antigens migrate to the lymph nodes and activate T cells.

The revised IFN-DC protocol has been demonstrated in research development to be a superior protocol for manufacturing DC vaccines. Compared with IL-4 DCs, IFN-DCs generated from human monocytes using GM-CSF and interferon (IFN)-α can induce differentiation in a shorter period of time [16]. Furthermore, compared with IL-4 DCs, IFN-DCs have been reported to be more capable of cross-presenting antigens to CD8^{+} T cells via major histocompatibility complex class I molecules after processing them into peptides [17]. Clinical trials have been conducted using IFN-DC vaccines for medullary thyroid tumor, advanced melanoma, and follicular lymphoma [18–20]. Thus, the combination of additives is particularly important because of the different characteristics of DCs generated by cytokines and adjuvants.

There are other problems associated with the manufacturing of DCs for clinical trials, such as the use of animal resource reagents that have a potential risk to infect cells with animal pathogens. Since safety is essential when applying DC vaccine therapy, the use of xeno-free reagents is recommended in addition to other cell therapies [21]. Recently, human platelet lysate (HPL) has been reported as an alternative to fetal bovine serum (FBS) for various cell types and cellular therapies; specifically, HPL has been used with mesenchymal stem cells to treat steroid-refractory acute graft-versus-host-disease (GVHD), endothelial colony-forming progenitor cells for transplantation into patients with cardiac diseases, and endothelial cells for tissue repair [22–24]. HPL contains a variety of factors, including cell proliferation-related (e.g., platelet-derived growth factor; PDGF, transforming growth factor-β; TGF-β), cell adhesion-related (e.g., sICAM-1, sVCAM-1), and inflammatory response-related (e.g., sCD40L) factors, that have favorable effectiveness in cell culture [25]. The use of HPL as an alternative to FBS when culturing IL-4 DCs has also been reported; however, there were no noticeable differences in endocytic activity, viability, and the expression of cell surface markers between the use of FBS and HPL [26]. Various interactions between monocytes and platelets have been reported, and the effects of platelets and their contents on monocytes and DCs have received much attention [27]. Therefore, we conducted IFN-DC vaccine manufacturing using a xeno-free medium and

HPL with a low adherent dish, with the results indicating a unique phenotype and function of the subsequent HPL-IFN-DCs.

2. Materials and Methods

2.1. Ethics

We performed DC generations in compliance with the Good Gene, Cellular, and Tissue-based Products Manufacturing Practice (GCTP). This study was evaluated and approved by the Ethical Committee of Kanazawa Medical University (approval number G131 and I489). All investigations were performed according to the Declaration of Helsinki, and all cells were obtained from patients after receiving the appropriate informed consent.

2.2. Cell Separation and Culture

2.2.1. Preparation of Peripheral Blood Mononuclear Cells (PBMCs)

PBMC-rich fractions were collected by a Spectra Optia® cell separator (Terumo BCT, Inc., Tokyo, Japan) using leukapheresis. Mononuclear cell-enriched fractions were separated from an apheresis product via density gradient centrifugation using Ficoll-Plaque Premium (Global Life Sciences Solutions USA LLC, Marlborough, MA, USA), and platelets were washed out with phosphate buffered saline (PBS).

2.2.2. Generation of IFN-DCs

PBMCs from the patients were suspended in serum-free medium DCO-K (Nissui Pharmaceutical Co., Ltd., Tokyo, Japan) supplemented with or without UltraGRO™-PURE GI GMP grade (hereinafter called "HPL"; AventaCell BioMedical Corp., Atlanta, GA, USA), which is an HPL reagent that has been approved as a material for regenerative medicine products by Pharmaceuticals and Medical Devices Agency in Japan; the PBMCs were then seeded into culture dishes for adherent cells. After 30 min, the non-adherent cells were washed out. The adherent cells were cultured in DCO-K medium that contained 100 ng/mL recombinant human GM-CSF (Miltenyi Biotec B.V. & Co. KG, Bergisch Gladbach, Germany) and 1 µg/mL PEGylated-IFN-α-2b (PEGINTRON®; MSD K.K., Tokyo, Japan) with or without 5% HPL for 3 days. The collected immature DCs were suspended in DCO-K medium with or without 5% HPL that contained 100 ng/mL GM-CSF, 1 µg/mL PEGINTRON®, 10 µg/mL OK-432 (Chugai Pharmaceutical Co., Ltd., Tokyo, Japan), 10 ng/mL PEG_2 (Kyowa Pharma Chemical Co., Ltd., Toyama, Japan), and 20 µg/mL tumor peptides such as Wilms tumor 1 (WT1; PEPTIDE INSTITUTE, Inc., Osaka, Japan) or melanoma antigen recognized by T cells 1 (MART-1; Medical & Biological Laboratories Co., Ltd., Nagoya, Japan). Hereinafter, this medium is referred to as the maturation cocktail. The cells suspended in the maturation cocktail were cultured in low adherent cell culture dishes and incubated for 24 h.

2.3. Cellular Morphology Observations

Cells that were adherent on day 1 were observed using a fluorescence microscope EVOS® FL Cell Imaging System (Thermo Fisher Scientific, Inc., Waltham, MA, USA) to observe cellular adherent state with a 10× objective lens magnification. Harvested mature DCs were observed using the all-in-one inverted fluorescence microscope BIOREVO BZ-9000 (KEYENCE CORPORATION., Osaka, Japan) for cellular morphology with a 40x objective lens magnification.

2.4. Cell Surface Marker Analysis

The following fluorochrome-conjugated mouse IgG anti-human monoclonal antibodies (mAbs) were used for the immunofluorescent staining: phycoerythrin (PE)-conjugated anti-CD11c mAbs (BioLegend, Inc., San Diego, CA, USA), fluorescein isothiocyanate (FITC)-conjugated anti-CD14 mAbs (eBioscience, Inc., San Diego, CA, USA), FITC-conjugated anti-CD40 mAbs (eBioscience, Inc.), PE-conjugated anti-CD56 mAbs (Beckman coulter, Inc., Brea, PA, USA), FITC-conjugated anti-CD80 mAbs (BD Biosciences, San Jase, CA, USA),

allophycocyanin (APC)-conjugated anti-CD83 mAbs (BioLegend, Inc.), PE-conjugated anti-CD86 mAbs (eBioscience, Inc.), PE-conjugated anti-CD197 (CCR7) mAbs (Research and Diagnostic Systems, Inc., Minneapolis, MN, USA), FITC-conjugated anti-HLA-ABC mAbs (BD Biosciences), PE-conjugated anti-HLA-DR mAbs (eBioscience, Inc.), FITC-conjugated anti-PD-L1 (BD Biosciences), and PE-conjugated anti-PD-L2 (BD Biosciences). FcR blocking reagent (Miltenyi Biotec B.V. & Co. KG) was added to the cells to block the non-specific binding of antibodies to DCs, and the cells were incubated for 10 min at room temperature. Antibodies were added to the cells, followed by 30 min of incubation at 4 °C in the dark. Then, they were washed with PBS and resuspended in PBS supplemented with 1% FBS and 7-amino-actinomycin D (7-AAD; BD Biosciences) for dead cell staining. The stained cells were analyzed with a BD FACSCalibur™ (BD Biosciences) or BD FACSCanto™II (BD Biosciences). The data were analyzed with the BD CellQuest Pro Software (BD Biosciences) or FlowJo™ Software (BD Biosciences).

2.5. Analysis of Endocytic and Proteolytic Activities

A total of 100 μg/mL FITC-Dextran (Molecular Probes, Inc., Eugene, OR, USA) or 10 μg/mL DQ ovalbumin (Molecular Probes, Inc.) was added to the maturation cocktail to measure endocytosis and proteolytic activity, respectively. After maturation, the collected DCs were washed with PBS twice, suspended in PBS supplemented with 1% FBS, and then analyzed by flow cytometry.

2.6. CTL Induction In Vitro

Immature DCs generated from HLA-A*02:01 PBMCs as described in 2.2.2. were matured using a maturation cocktail with the addition of 20 μg/mL HLA-A*02:01 MART-1 peptides (ELAGIGILTV; Medical & Biological Laboratories Co., Ltd., Nagoya, Japan). After 24 h, DCs were collected as stimulator cells, divided into aliquots, and cryopreserved. CD8$^+$ T cells were separated from HLA-A*02:01-autologous PBMCs using CD8 microbeads (Miltenyi Biotec B.V. & Co. KG, Bergisch Gladbach, Germany) and were applied as responder cells. The stimulator and responder cells were co-cultured in a 96-well U-bottom plate at a ratio of 1:10 in AIM-V medium (Thermo Fisher Scientific, Inc., Waltham, MA, USA) supplemented with 5 ng/mL IL-2 (PeproTech, Inc., Rocky Hill, NJ, USA), 5 ng/mL IL-7 (Research and Diagnostic Systems, Inc.), 10 ng/mL IL-15 (PeproTech, Inc., Rocky Hill, NJ, USA), and 50 μg/mL 2-mercapto-ethanol (Bio-Rad Laboratories, Inc., Hercules, CA, USA) as the stimulation medium. After 3 days of cultivation, AIM-V media supplemented with 10% human AB serum (Biowest, Nuaillé, France) and 50 μg/mL 2-mercapto-ethanol were added as expansion medium. Thereafter, DC stimulation and cell expansion were repeated twice with a 3-day interval. The co-cultured cells were collected 14 days after the first stimulation, and 1×10^6 cells were stained with FITC-conjugated anti-CD8 (Beckman Coulter, Inc., Brea, PA, USA), APC-conjugated anti-CD3 (eBioscience, Inc., San Diego, CA, USA), and PE-conjugated T-Select HLA-A*02:01 MART-1 Tetramer-ELAGIGILTV (Medical & Biological Laboratories Co., Ltd., Nagoya, Japan) to detect the MART-1-specific CTLs. Dead cells were excluded by 7-AAD staining in a flow cytometry analysis.

2.7. Detection of Cytokine Production

The collected mature IFN-DCs were seeded at a concentration of 1×10^6 cells/mL, transferred into DCO-K serum-free medium (without HPL), then incubated at 37 °C for 24 h. The culture supernatants were subjected to a Bio-Plex or enzyme-linked immunosorbent assay (ELISA) analysis to quantify the following cytokines: Bio-Plex: IL-6, IL-10, IL-12 (p70), IFN-γ, and TNF-α; ELISA: transforming growth factor (TGF) -β1. Basal cytokine levels were also analyzed. All measurements were performed in duplicate using a Bio-Plex assay kit (Bio-Rad Laboratories, Inc., Hercules, CA, USA) and a Human TGF-beta 1 Quantikine ELISA Kit (Research and Diagnostic Systems, Inc., Minneapolis, MN, USA) according to the protocol of each kit.

2.8. Enzyme-Linked Immunosorbent Spot (ELISpot) Assay

The ELISpot assays were performed to examine MART-1-specific IFN-γ production using a human IFN-γ ELISpot PLUS kit (Mabtech AB, Nacka Strand, Sweden) according to the manufacturer's instructions. Briefly, the cells had been cultured for 21 days that were collected and suspended in AIM-V with 10% FBS and 20 μg/mL HLA-A*02:01 MART-1 peptides (ELAGIGILTV; Medical & Biological Laboratories Co., Ltd., Nagoya, Japan) or 20 μg/mL HLA-A*02:01 HIV gag peptides (SLYNTVATL; Medical & Biological Laboratories Co., Ltd., Nagoya, Japan; used as a negative control) to detect MART-1$^+$ CTL induction on day 21. These CTLs were placed in 96-well ELISpot plates precoated with IFN-γ monoclonal antibodies at a concentration of 1×10^5 cells per well. The antibody reactions and staining were performed according to the kit protocol. Then, the emerged spots were counted by an automated ELISpot reader (AID ELISpot Reader Classic ELR 07; Autoimmun Diagnostika GmbH, Strassberg, Germany).

2.9. Statistical Analysis

The Wilcoxon signed-rank test was used to compare the differences between IFN-DCs and HPL-IFN-DCs. All statistical analyses were performed using IBM SPSS Statistics software version 24 (IBM Japan, Ltd., Tokyo, Japan). Differences were considered statistically significant at a *p*-value < 0.05.

3. Results

3.1. Generation of IFN-DCs Using Serum-Free Medium Supplemented with HPL

DCs were produced from the patients' PBMCs in the absence or presence of HPL as described in 2.2.2. (Figure 1a). After cell adhesion on day 1, microscopic observation indicated that many lymphocyte-like small cells remained in the absence of HPL (Figure 1b, upper left panel). Conversely, there was little contamination of lymphocyte-like small cells in the presence of HPL (Figure 1b, upper right panel). Hereinafter, DCs cultured in the absence or presence of HPL are referred to as "IFN-DCs" or "HPL-IFN-DCs," respectively. Dendritic-like structures were observed in both IFN-DCs and HPL-IFN-DCs under microscopy (Figure 1b, lower panel). The viability and DC/monocyte recovery rates were significantly higher in HPL-IFN-DCs than in IFN-DCs (Figure 1c; median viability: IFN-DCs, 84.2%; HPL-IFN-DCs, 95.5%; yield: IFN-DCs, 14.1%; HPL-IFN-DCs, 25.4%). Additionally, the flow cytometric analyses indicated a lower rate of lymphocyte contamination in the HPL-IFN-DCs. The adhesion procedure followed by cell culturing demonstrated a far superior DC purity in the presence of HPL than in the absence of HPL (Figure 1c; median purity: IFN-DCs, 83.1%; HPL-IFN-DCs, 99.1%). These results reflect the higher viability, yield, and purity of HPL-IFN-DCs compared with IFN-DCs.
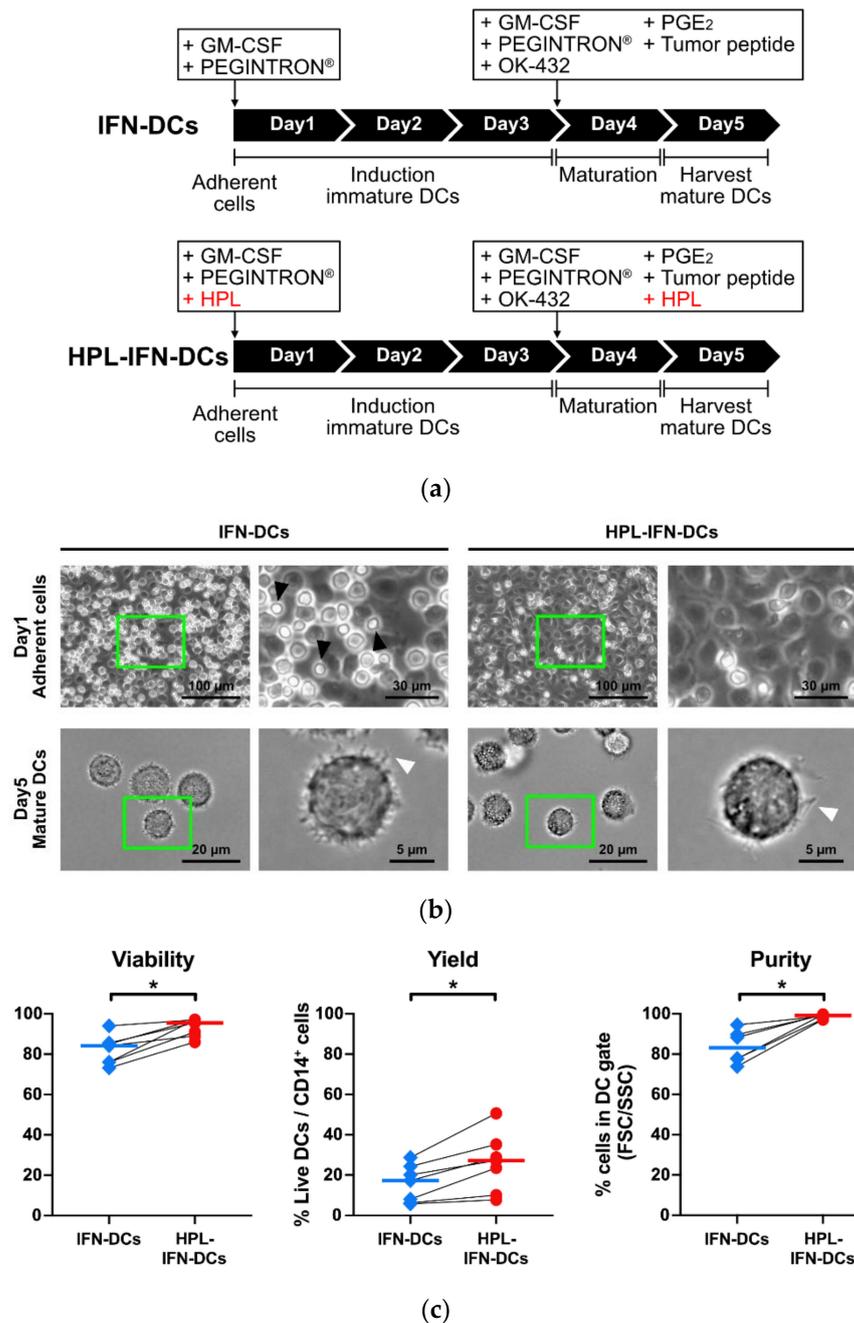
(**a**)

(**b**)

(**c**)

Figure 1. The viability, yield, and purity in IFN-DCs and HPL-IFN-DCs. (**a**) Adherent cells were cultured in DCO-K medium supplemented with or without 5% HPL, as described in the Materials and Methods. In the presence of the HPL conditioning regimen, HPL was continuously added through monocyte selection and harvested DCs. (**b**) The upper panels display micrographs of cells seeded on adherent dishes (magnification: ×10, scale bar: 100 and 30 μm). The black arrowheads indicate small cells, such as lymphocytes. The lower panels display micrographs of the harvested mature DCs in a glass bottom dish (magnification: ×40, scale bar: 20 and 5 μm). The white arrowheads indicate dendrite-like structures. A partial close-up is shown to the right of each photo (green squares). (**c**) Dead cells were measured by trypan blue staining to compare the viability and yield of the DC/monocyte ratio. DC purity was measured by flow cytometry. The gated cells from FSC and SSC, excluding the lymphocyte fraction, were defined as DCs (viability and yield, *n* = 7; purity, *n* = 6). The bold horizontal bars in the graphs indicate the median of each parameter. * *p* < 0.05.

3.2. Phenotypic Comparison between IFN-DCs and HPL-IFN-DCs

To determine the effect of HPL on the IFN-DC phenotype, we used flow cytometry to analyze the following cell surface markers that had been reported in previous monocyte-derived DC studies [28,29]: CD11c, CD14, CD40, CD56, CD80, CD83, CD86, CCR7, HLA-ABC, HLA-DR, PD-L1, and PD-L2 (Figure 2). Notably, compared with IFN-DCs, HPL-IFN-DCs expressed higher levels of CD11c (median percentage of positive cells: 98.3% in IFN-DCs; 99.9% in HPL-IFN-DCs), CD14 (35.8% in IFN-DCs; 83.6% in HPL-IFN-DCs), CD56 (37.6% in IFN-DCs; 68.4% in HPL-IFN-DCs), and CCR7 (10.3% in IFN-DCs; 37.8% in HPL-IFN-DCs). Conversely, HPL-IFN-DCs displayed significantly decreased expressions of the HLA co-stimulatory molecules CD40 (98.6% in IFN-DCs; 66.9% in HPL-IFN-DCs) and CD80 (84.0% in IFN-DCs; 33.1% in HPL-IFN-DCs) and the maturation marker CD83 (86.8% in IFN-DCs; 64.2% in HPL-IFN-DCs). HLA-DR expression, which is responsible for antigen presentation to helper T cells, was also slightly down-regulated in HPL-IFN-DCs (99.8% in IFN-DCs; 92.7% in HPL-IFN-DCs). There were no significant differences between IFN-DCs and HPL-IFN-DCs regarding the expressions of CD86, a co-stimulatory molecule important for T cell activation (99.6% in IFN-DCs; 99.6% in HPL-IFN-DCs); HLA-ABC, an antigen presentation to killer T cells (100% in IFN-DCs; 100% in HPL-IFN-DCs); and PD-L1 and PD-L2, immune checkpoint molecules (PD-L1+: 73.6% in IFN-DCs; 94.6% in HPL-IFN-DCs; and PD-L2+: 13.9% in IFN-DCs; 23.5% in HPL-IFN-DCs).
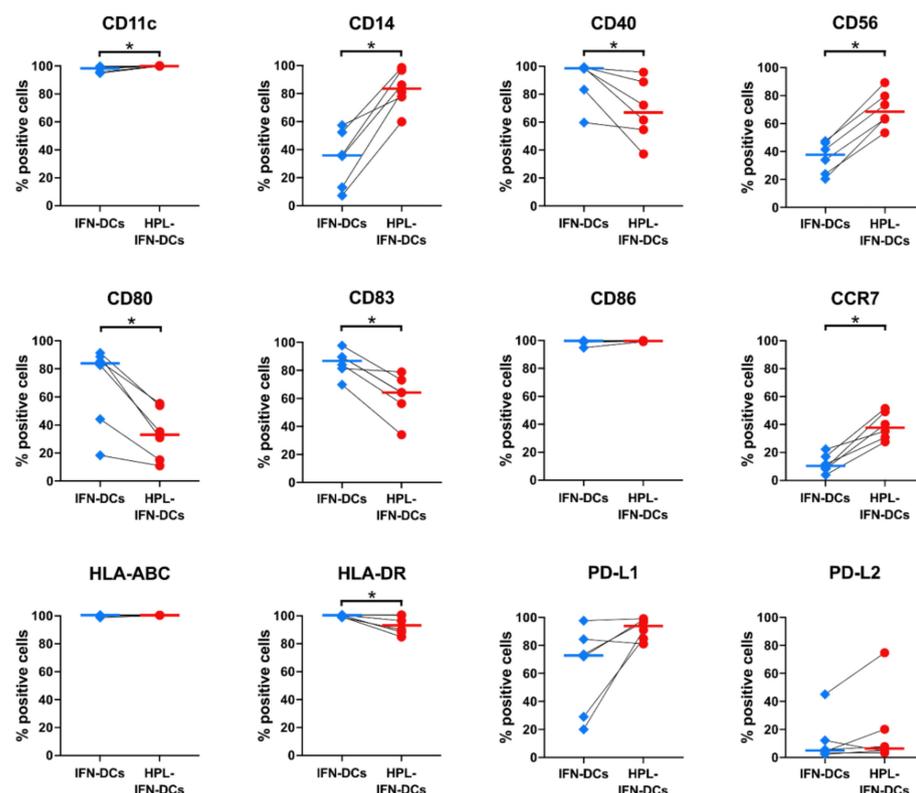

Figure 2. Phenotypic comparison between IFN-DCs and HPL-IFN-DCs. After harvesting IFN-DCs and HPL-IFN-DCs prepared from the same donors, the DCs were stained with antibodies for DC markers and analyzed using flow cytometry (*n* = 6). The bold horizontal bars in the graphs indicate the median of each parameter. * *p* < 0.05.

3.3. HPL-IFN-DCs Are Highly Capable of Inducing Antigen-Specific CTLs

To investigate the antigen-presenting abilities of generated DCs to CD8+ T cells, antigen-specific CTLs were sensitized with IFN-DCs using a MART-1 peptide. MART-1-specific CTLs could be detected by a MART-1 tetramer analysis on days 14 and 21.

HPL-IFN-DCs showed significantly higher MART-1-specific CTL induction than IFN-DCs on day 14 (Figure 3a,b; median MART-1 tetramer$^+$ CTLs on day 14: IFN-DCs, 0.29%; HPL-IFN-DCs, 2.88%; $n = 6$). Surprisingly, many more MART-1 tetramer$^+$ CTLs were found on day 21 in vitro (Figure 3b; median percentage MART-1 tetramer$^+$ CTLs on day 21: IFN-DCs, 1.36%; HPL-IFN-DCs, 9.33%). The average numbers of MART-1 tetramer$^+$ CTLs had time-dependently increased on day 21 compared with that on day 14, which is demonstrated in the growth curve in Figure 3c. The number of MART-1 tetramer$^+$ CTLs increased significantly in both IFN-DCs and HPL-IFN-DCs, from $9.33 \times 10^4 \pm 1.07 \times 10^5$ and $4.41 \times 10^5 \pm 4.72 \times 10^5$ cells on day 14, respectively, to $5.69 \times 10^5 \pm 5.76 \times 10^5$ cells (IFN-DCs) and $1.62 \times 10^6 \pm 6.42 \times 10^5$ cells (HPL-IFN-DCs) on day 21 ($n = 6$). This quantitative analysis indicates that HPL-IFN-DCs had a significantly greater potential to present antigens to CD8$^+$ T cells than IFN-DCs.
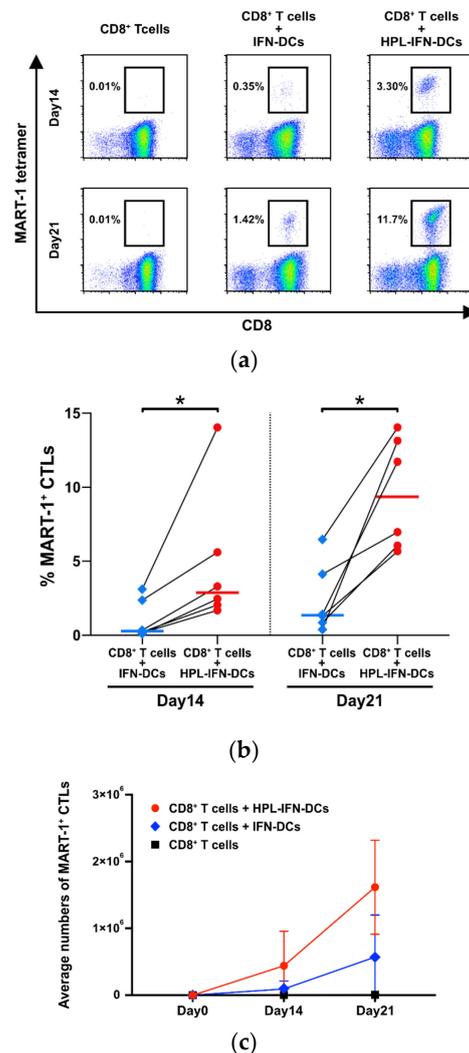

(a)

(b)

(c)

Figure 3. HPL-IFN-DCs for MART-1-specific CTL induction. IFN-DCs or HPL-IFN-DCs were co-cultured with autologous T cells at a ratio of E:T = 1:10. (**a**) Fourteen or 21 days after the start of co-culturing, MART-1-specific CTLs were detected by CD3, CD8, and MART-1 positive gates via flow cytometry ($n = 6$). These dot plots show a representative example. The percentages in the panels indicate the MART-1 tetramer$^+$ ratio in CD8$^+$ T cells. (**b**) The graph shows the ratio of MART-1 CTLs co-cultured with either IFN-DCs or HPL-IFN-DCs on days 14 and 21. The bold horizontal bars indicate the median of each parameter ($n = 6$). * $p < 0.05$. (**c**) This line graph shows the number of MART-1$^+$ CTLs in the culture period (mean $\pm$ standard deviation). The vertical axis represents the average number of cells ($n = 6$).

3.4. CTLs Induced by IFN-DCs or HPL-IFN-DCs Produced IFN-γ in Response to MART-1 Peptides

Although HPL-IFN-DCs significantly induced CTLs, it remains unclear whether the sensitized CTLs would be functional. IFN-γ production by CTLs is crucial for the efficacy of the DC vaccine. The frequency of IFN-γ production from CTLs was calculated in a MART-1-specific manner using ELISpot assays. IFN-γ spots by MART-1 peptide could be specifically detected in T cells co-cultured with either IFN-DCs or HPL-IFN-DCs (Figure 4a; upper panels). Interestingly, there were more IFN-γ-positive spots in CD8$^+$ T cells co-cultured with HPL-IFN-DCs (median number of spots: 505.8) than in those co-cultured with IFN-DCs (304.0). This result was consistent with the trend in CTL induction shown in Figures 3b and 4b (*n* = 6). There was no significant difference in the number of spots between the MART-1 peptide (23.8) and the negative control HIV peptide (25.0) in CD8$^+$ T cells cultured alone. Moreover, both CD8$^+$ T cells co-cultured with IFN-DCs and those co-cultured with HPL-IFN-DCs showed little responsiveness to HIV peptides, indicating that these cells produced IFN-γ in a MART-1-specific manner (12.3 in IFN-DCs; 37.0 in HPL-IFN-DCs).
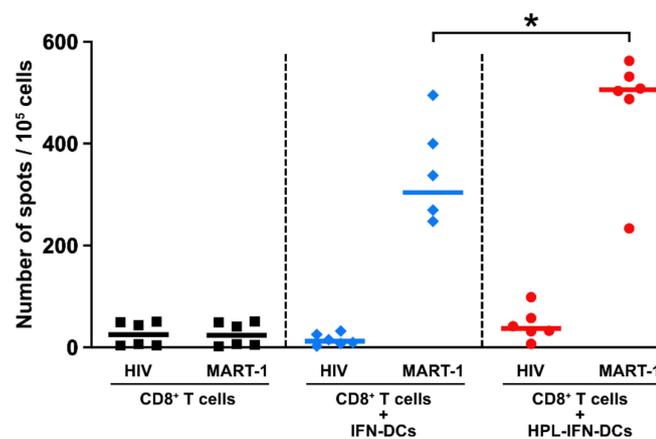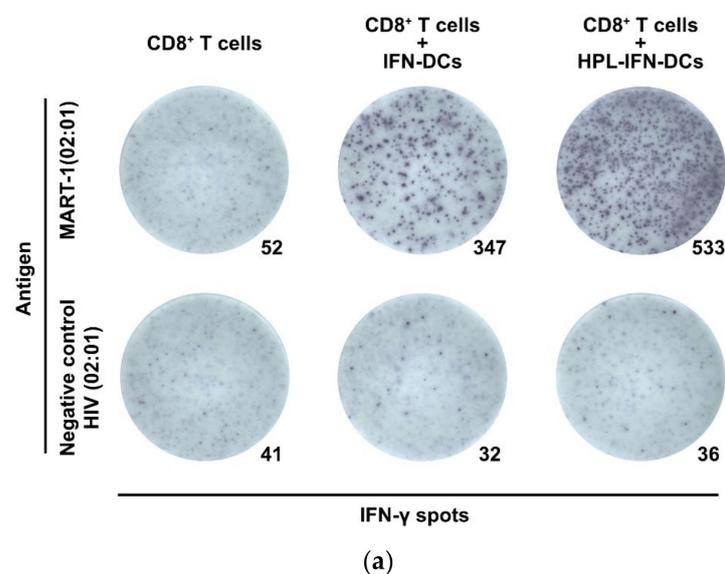

(**a**)

(**b**)

Figure 4. IFN-γ production in response to MART-1 peptide in CTLs. (**a**) The representative ELISpot assays highlight IFN-γ-specific spots upon CTL stimulation with MART-1 peptides (ELAGIGILTV) or HIV peptides as the negative control (*n* = 6). (**b**) The scatter plots indicate the number of spots for each well. The bold horizontal bars in the graphs indicate the median of each parameter. * *p* < 0.05.

3.5. HPL Upregulated the Endocytic and Proteolytic Activities of IFN-DCs

Figures 3 and 4 show that HPL-IFN-DCs had the ability to induce strong antigen-specific and functional CTLs. To confirm whether the addition of HPL alters functions other than CTL induction capacity, we investigated endocytic and proteolytic activities, which are important functions of APCs. FITC-dextran or DQ ovalbumin was added to the maturation cocktail and were detected by flow cytometry. Interestingly, the Δ median fluorescent intensity (ΔMFI) values of FITC-Dextran (17.1 in IFN-DCs; 68.0 in HPL-IFN-DCs) and DQ ovalbumin (270.9 in IFN-DCs; 589.7 in HPL-IFN-DCs) were significantly higher in HPL-IFN-DCs than in IFN-DCs, as shown in Figure 5.
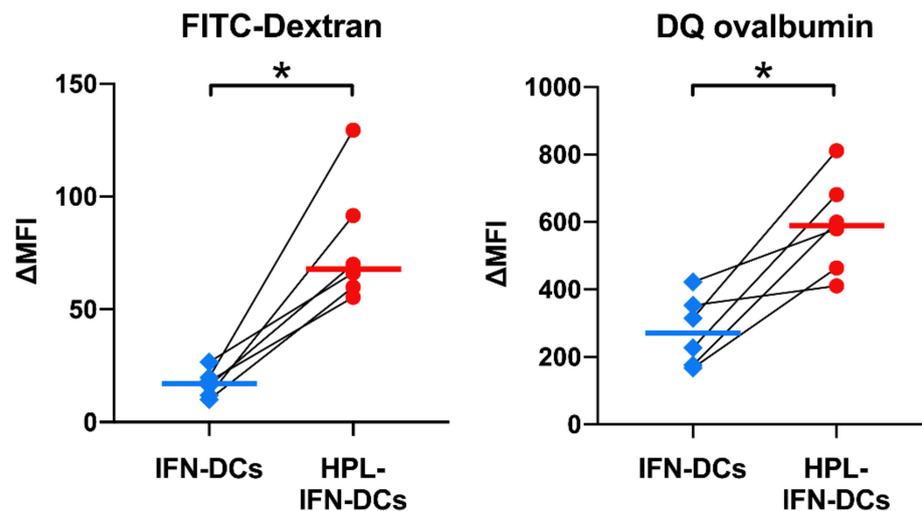

Figure 5. Endocytic and proteolytic activity of HPL-IFN-DCs and IFN-DCs. DCs were incubated with FITC-Dextran to measure antigen endocytosis or DQ ovalbumin to measure proteolytic activity in the maturation cocktail at the time of maturation. These cells were washed after incubating for 24 h, and the fluorescence intensity was measured with flow cytometry ($n = 6$). Δ median fluorescence intensity (ΔMFI) was obtained after subtracting the control incubated with DMSO. The bold horizontal bars in the graphs show the median of each parameter. * $p < 0.05$.

3.6. Compared with IFN-DCs, HPL-IFN-DCs Showed Higher IL-6, IL-10, and TNF-α Production Levels

To evaluate the ability of HPL-IFN-DCs to produce the cytokines involved in antigen presentation, the IL-6, IL-10, IL-12 (p70), IFN-γ, TNF-α, and TGF-β1 levels were measured with a multiplex or ELISA (Figure 6). To measure the cytokines produced from DCs under steady conditions without HPL interference, the prepared IFN-DCs and HPL-IFN-DCs were incubated in DCO-K medium only. DCO-K medium with or without 5% HPL were confirmed to contain undetectable cytokine levels (each cytokine level indicated less than 1 pg/mL in both medium conditions, besides TGF-β1, 3869.5 pg/mL in DCO-K with 5% HPL); therefore, we performed incubation with DCO-K medium only to exclude its effect. Compared with IFN-DCs, HPL-IFN-DCs secreted more IL-6 (median amount: 302.3 pg/mL in IFN-DCs; 2883.0 pg/mL in HPL-IFN-DCs), IL-10 (11.47 pg/mL in IFN-DCs; 132.7 pg/mL in HPL-IFN-DCs), and TNF-α (412.5 pg/mL in IFN-DCs; 1144.4 pg/mL in HPL-IFN-DCs). A very low amount of IL-12 (p70) was detected from the IFN-DCs and HPL-IFN-DCs (median amount: 1.1 pg/mL in IFN-DCs; 0.18 pg/mL in HPL-IFN-DCs); this difference was significant. Conversely, very low levels of both IFN-γ and TGF-β1 were detected in IFN-DCs and HPL-IFN-DCs with no significant difference between the two types of DCs (median IFN-γ level: 0.59 pg/mL in IFN-DCs; 0.38 pg/mL in HPL-IFN-DCs; median TGF-β1 level: 8.02 pg/mL in IFN-DCs; 9.38 pg/mL in HPL-IFN-DCs).
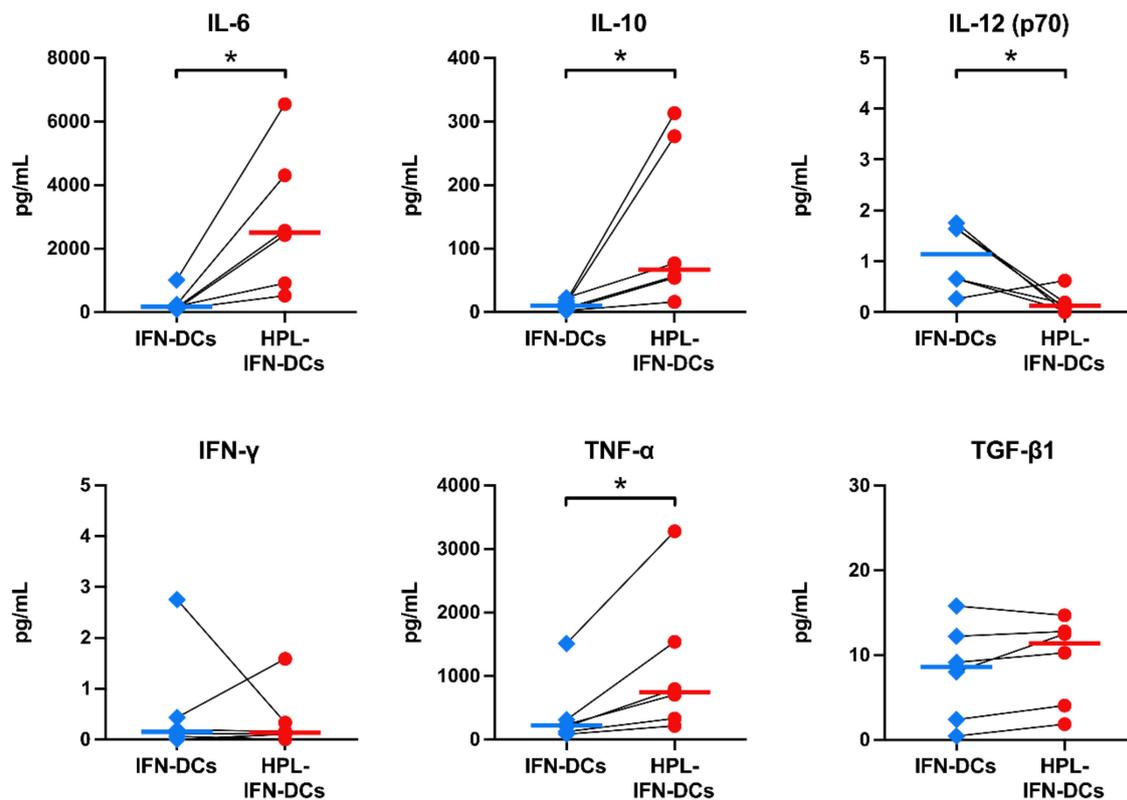
Figure 6. Levels of cytokine production of HPL-IFN-DCs compared to IFN-DCs. Cytokine production was measured in the supernatants collected from IFN-DCs or HPL-IFN-DCs in DCO-K serum-free medium for 24 h. The IL-6, IL-10, IL-12 (p70), IFN-γ, and TNF-α levels were determined with a Bio-Plex multiplex assay, and the amount of TGF-β1 was determined by an ELISA (*n* = 6). The bold horizontal bars in the graphs show the median of each parameter. * *p* < 0.05.

4. Discussion

This study showed that HPL could potentiate IFN-DCs with enhanced antigen presentation, endocytosis, and proteolysis during differentiation and maturation from monocytes; this procedure resulted in high viability, yield, and purity.

For the initial validation of the additives, IFN-DCs were cultured in DCO-K medium, DCO-K with 5% human AB serum, or DCO-K with 5% HPL (Table S1). The viability and yield of IFN-DCs in DCO-K with human AB serum were the lowest among the groups (Table S1). PDGF, which is more abundant in HPL than in human AB serum, has been reported to inhibit apoptosis and is presumed to contribute to increased viability [30,31]. Moreover, IFN-DCs with AB serum were not found to have a remarkable change in surface markers in HPL-IFN-DCs when compared with IFN-DCs with DCO-K-only (Figure S1). These analyses lead to focusing on HPL-IFN-DCs with unique surface markers, high survival, and yield.

To determine the optimal HPL ratio in the medium, concentrations of 1%, 5%, and 10% were compared with the non-additional control. Despite a few differences, 5% was adopted as the optimal HPL content ratio for further study based on the DC/monocyte yield, cell viability, and the expressions of representative surface markers, such as CD86 and HLA-ABC (Figure S2). Because HPL contains factors that promote monocyte adhesion, such as ICAM-1 and VCAM-1 [25,32], HPL appears to effectively promote the adhesion of monocytes to cell culture dishes, consequently reducing the rate of non-adhesive lymphocyte contamination (Figure 1c). Moreover, apoptosis is inhibited by exosomes contained in platelet-rich plasma and the raw material of HPL [33]; therefore, a similar effect of HPL may lead to a high viability with an increase in the yield of HPL-IFN-DCs (Figure 1c). The revised manufacturing protocol using HPL would be expected to reduce the number of

monocytes collected from patients; thus, highly valuable vaccine products would achieve clinical efficiency for cancer vaccination.

As shown in Figure 2, IFN-DCs cultured in serum-free medium showed similar cell surface markers as previously reported on IFN-α-induced DCs [18]. However, HPL-IFN-DCs displayed a unique phenotype with a conservative expression of CD14, a monocyte marker, and lower expressions of DC maturation markers, such as CD40, CD80, and CD83; this phenotype appears to be similar to that of so-called semi-mature DCs [34]. Additionally, similar to semi-mature DCs, HPL-IFN-DCs also displayed cytokine profiles with higher levels of IL-6 and IL-10 (Figure 6). Semi-mature DCs are known to cause immune tolerance [35]. However, unlike semi-mature DCs, HPL-IFN-DCs displayed high CD86 and HLA-DR expression levels and only produced small amounts of TGF-β1. Since immature DCs spontaneously mature and migrate into the lymph nodes after administration, as reported in rhesus monkey and chimpanzee studies [36,37], the degree of maturation of DCs likely depends on the surrounding conditions. After intradermal injection into rhesus monkeys, immature DCs completely migrated out of the skin, whereas mature DCs tended to remain in the dermis [36]. Although it is difficult to determine the maturation degree based only on the phenotyping of HPL-IFN-DCs, the adoption of maturity as a release criterion for a DC vaccine is controversial. CCR7, which is required for DC migration to the lymph nodes, was hardly expressed by conventional IFN-DCs [38]; however, its expression was enhanced in HPL-IFN-DCs (Figure 2). Based on in vitro chemotaxis experiments using a transwell system to examine DCs migration toward CCL19, CCR7 expression plays a critical role in the migration of DCs [39]. This phenotype is expected to increase the rate of migration to the lymph nodes because of the intradermal administration of HPL-IFN-DCs. Additionally, HPL-IFN-DCs showed higher expression of the natural killer cell marker CD56 (Figure 2). Although conventional IFN-DCs partially expressing CD56 resembled CD56^{+} IFN-DCs with cytotoxic activity [16,18], this activity was not found in HPL-IFN-DCs (Figure S3). Conversely, high PD-L1 expression, an immune checkpoint molecule, was detected in both IFN-DCs and HPL-IFN-DCs (Figure 2). PD-L1 is generally known to act suppressively on T cell activation [40]. Furthermore, PD-L1 expression is upregulated during antigen uptake in cDC1 [41], and PD-L expression on DCs is involved in promoting CD4^{+}CD25^{+}FoxP3^{+} regulatory T cell expansion and function [42]. Ex-vivo-generated HPL-IFN-DCs can be furnished with tumor antigens exploiting their antigen-specific qualities in Figure 3; therefore, it is possible that HPL-IFN-DCs expressing PD-L1 would improve potency to promote cytotoxic and long-lasting immunity under immunosuppressive regulation.

The most remarkable result in our study was that HPL-IFN-DCs showed potent antigen-specific CTL induction abilities (Figure 3). Han P. et al. recently reported that P-selectin in platelets affects P-selectin glycoprotein ligand 1 (PSGL1) in monocytes, and co-culturing of monocytes and platelets enhances cross-presentation abilities [43]. Although it is not clear whether P-selectin is present in HPL, this report supports the evidence that HPL-IFN-DCs would have a high antigen-specific CTL induction capacity. Additionally, we speculate that this high antigen-presenting capacity is due to an enhanced ability to take up and process antigens. The high endocytic and proteolytic capacities of HPL-IFN-DCs (Figure 5) would likely be enhanced by abundant cytokines contained in HPL. Low concentrations of TNF-α and GM-CSF act synergistically in macrophages, leading to a dramatic upregulation of endocytic activity [44]. In addition, it is speculated that epidermal growth factor (EGF) contained in HPL, which is known to stimulate EGF receptor on DCs, would promote endocytosis [45]. Because the experiments on antigen presentation, antigen uptake, and processing are independent analyses, we did not prove a sequential cross-presentation cascade. Future validation is needed to determine the cross-presentation ability in HPL-IFN-DCs. Cytokines produced by HPL-IFN-DCs may also support the antigen-presenting capability. As shown in Figure 6, HPL-IFN-DCs produced higher levels of IL-6, IL-10, and TNF-α than IFN-DCs. IL-6 is required in the early stages of CTL induction, and proliferation is subsequently promoted by IL-2 [46]. IL-10 acts on both sides,

functioning as both an immunosuppressive agent [47] and as a direct enhancer for the proliferation and cytotoxic function of human papillomavirus (HPV)-specific CD8^{+} T cells with an increase in intracellular perforin levels [48]. IL-10 injection in mice was shown to enhance anti-tumor immunity immediately after DC vaccine administration [49]. These reports indicate that IL-10 actively plays an important role against acquired immunity dependent on the optimized condition rather than merely regulating via suppression. Elevated TNF-α levels (Figure 6) have a potential role to improve IL-2 responsiveness and promote T cell proliferation [50]. Our results indicated that IL-12 (p70) production is lower in both IFN-DCs and HPL IFN-DCs (Figure 6). Increased IL-12 production by DCs is an important step in the process of CTL priming, and IL-12 is required for the maximal expression of IFN-γ-secreting CTLs in vitro [51]. Our finding indicated that HPL-IFN-DCs could induce a high level of IFN-γ-producing CTLs despite the low production of IL-12, suggesting that CTLs can be activated in a pathway independent of IL-12 (Figure 4). Conversely, both HPL-IFN-DCs and IFN-DCs displayed lower levels of TGF-β1, which downregulates the antigen presentation function [52].

One of the remaining questions is whether HPL-IFN-DCs are close to any DC subset or monocyte-derived cell population in vivo. CD14-positive DCs have been identified in dermis-expressing markers such as DC-SIGN and CX3CR1 [5,53]. Interestingly, these markers were slightly upregulated in HPL-IFN-DCs compared with IFN-DCs (Figure S4). The phenotype of HPL-IFN-DCs is more similar to that of CD14^{+} DCs differentiated from CD34^{+} hematopoietic stem cells than that of dermal CD14^{+} DCs in vivo [54]. Nevertheless, HPL-IFN-DCs displayed a higher capability of inducing differentiation into potent CTL effectors than both Langerhans cells and CD14^{+} DCs. Exposure to HPL markedly increased the expression of CD141 on HPL-IFN-DCs (Figure S4); this marker is characteristically expressed on cDC1 with a high antigen-presenting capacity. Since XCR1 and CLEC9A are also expressed together in these subsets in human blood [4], the expressions of XCR1 and CLEC9A were also examined in HPL-IFN-DCs but were not detected (Figure S4). Because gene expression differs at the single-cell level even in a population of the same phenotype, the ability to determine the exact subtype based solely on surface antigen analysis is limited. HPL components might affect monocytes that differentiate into a novel type of *DCs* mimicking CD14^{+} DCs; therefore, a comprehensive analysis of mRNA expression per single cell can be used to determine the single-cell RNA sequence of HPL-IFN-DCs to understand the differentiation genealogy of the monocyte and functional pathways upregulated by HPL. Such analyses of HPL-IFN-DCs are expected to deepen the understanding of adaptive immunity and contribute to the development of DC vaccination against refractory cancers and infectious diseases to improve human healthcare.

5. Conclusions

In the presence of HPL, IFN-DCs displayed higher viability, yield, and purity, showing a unique phenotype with increased expressions of CD14, CD56, and CCR7. HPL-IFN-DCs induced an extremely high level of antigen-specific CTLs that secreted high levels of IFN-γ. Additionally, antigen endocytosis and proteolytic activities were observed in HPL-IFN-DCs. Our findings suggest that ex-vivo-generated HPL-IFN-DCs would exhibit a novel monocyte-derived DC type with high endocytic and proteolytic activities, which provides insights into a unique type of monocyte-derived DCs exposed to HPL. Further gene expression levels in HPL-IFN-DCs must be analyzed to determine the genealogy of the monocyte lineage for future vaccination therapies.

6. Patents

S.S. and T.K. are inventors of the patent for manufacturing an IFN-DC vaccine (WO2016/148179).

Supplementary Materials: The following are available online at https://www.mdpi.com/2076-393X/9/1/10/s1: Table S1: Viability and yield of IFN-DCs in DCO-K only, with human AB serum, and with HPL conditions.; Figure S1: Panels of surface marker expression on IFN-DCs either with human

AB serum or with HPL in DCO-K medium.; Figure S2: Verification of the optimal concentration of HPL for IFN-DC generation.; Figure S3: HPL-IFN-DCs have little tumor killing activity.; Figure S4: The expressions of cell surface markers associated with dermal DCs.

References

1. Banchereau, J.; Steinman, R.M. Dendritic Cells and the Control of Immunity. *Nature* **1998**, *392*, 245–252. [CrossRef] [PubMed]
2. Granot, T.; Senda, T.; Carpenter, D.J.; Matsuoka, N.; Weiner, J.; Gordon, C.L.; Miron, M.; Kumar, B.V.; Griesemer, A.; Ho, S.H.; et al. Dendritic Cells Display Subset and Tissue-Specific Maturation Dynamics over Human Life. *Immunity* **2017**, *46*, 504–515. [CrossRef] [PubMed]
3. Collin, M.; McGovern, N.; Haniffa, M. Human Dendritic Cell Subsets. *Immunology* **2013**, *140*, 22–30. [CrossRef] [PubMed]
4. Villani, A.C.; Satija, R.; Reynolds, G.; Sarkizova, S.; Shekhar, K.; Fletcher, J.; Griesbeck, M.; Butler, A.; Zheng, S.; Lazo, S.; et al. Single-Cell RNA-Seq Reveals New Types of Human Blood Dendritic Cells, Monocytes, and Progenitors. *Science* **2017**, *356*. [CrossRef]
5. McGovern, N.; Schlitzer, A.; Gunawan, M.; Jardine, L.; Shin, A.; Poyner, E.; Green, K.; Dickinson, R.; Wang, X.N.; Low, D.; et al. Human Dermal CD14+ Cells Are a Transient Population of Monocyte-Derived Macrophages. *Immunity* **2014**, *41*, 465–477. [CrossRef]
6. Wylie, B.; Macri, C.; Mintern, J.D.; Waithman, J. Dendritic Cells and Cancer: From Biology to Therapeutic Intervention. *Cancers* **2019**, *11*, 521. [CrossRef]
7. Akagawa, K.S.; Takasuka, N.; Nozaki, Y.; Komuro, I.; Azuma, M.; Ueda, M.; Naito, M.; Takahashi, K. Generation of CD1+RelB+ Dendritic Cells and Tartrate-Resistant Acid Phosphatase-Positive Osteoclast-Like Multinucleated Giant Cells from Human Monocytes. *Blood* **1996**, *88*, 4029–4039. [CrossRef]
8. Fu, C.; Jiang, A. Dendritic Cells and CD8 T Cell Immunity in Tumor Microenvironment. *Front. Immunol.* **2018**, *9*, 3059. [CrossRef]
9. Koya, T.; Date, I.; Kawaguchi, H.; Watanabe, A.; Sakamoto, T.; Togi, M.; Kato, T.; Yoshida, K.; Kojima, S.; Yanagisawa, R.; et al. Dendritic Cells Pre-Pulsed with Wilms' Tumor 1 in Optimized Culture for Cancer Vaccination. *Pharmaceutics* **2020**, *12*, 305. [CrossRef]
10. Yanagisawa, R.; Koizumi, T.; Koya, T.; Sano, K.; Koido, S.; Nagai, K.; Kobayashi, M.; Okamoto, M.; Sugiyama, H.; Shimodaira, S. WT1-Pulsed Dendritic Cell Vaccine Combined with Chemotherapy for Resected Pancreatic Cancer in a Phase I Study. *Anticancer Res.* **2018**, *38*, 2217–2225. [CrossRef]
11. Pierret, L.; Wilgenhof, S.; Corthals, J.; Roelandt, T.; Thielemans, K.; Neyns, B. Correlation between Prior Therapeutic Dendritic Cell Vaccination and the Outcome of Patients with Metastatic Melanoma Treated with Ipilimumab. *J. Clin. Oncol.* **2009**, *27*, e20006. [CrossRef]

12. Nesselhut, J.; Marx, D.; Lange, H.; Regalo, G.; Cillien, N.; Chang, R.Y.; Nesselhut, T. Systemic Treatment with Anti-PD-1 Antibody Nivolumab in Combination with Vaccine Therapy in Advanced Pancreatic Cancer. *J. Clin. Oncol.* **2016**, *34*, 3092. [CrossRef]

13. Tanyi, J.L.; Bobisse, S.; Ophir, E.; Tuyaerts, S.; Roberti, A.; Genolet, R.; Baumgartner, P.; Stevenson, B.J.; Iseli, C.; Dangaj, D.; et al. Personalized Cancer Vaccine Effectively Mobilizes Antitumor T Cell Immunity in Ovarian Cancer. *Sci. Transl. Med.* **2018**, *10*, eaao5931. [CrossRef] [PubMed]

14. Li, D.Y.; Gu, C.; Min, J.; Chu, Z.H.; Ou, Q.J. Maturation Induction of Human Peripheral Blood Mononuclear Cell-Derived Dendritic Cells. *Exp. Ther. Med.* **2012**, *4*, 131–134. [CrossRef] [PubMed]

15. Shimodaira, S.; Yanagisawa, R.; Koya, T.; Hirabayashi, K.; Higuchi, Y.; Sakamoto, T.; Togi, M.; Kato, T.; Kobayashi, T.; Koizumi, T.; et al. In Vivo Administration of Recombinant Human Granulocyte Colony-Stimulating Factor Increases the Immune Effectiveness of Dendritic Cell-Based Cancer Vaccination. *Vaccines* **2019**, *7*, 120. [CrossRef]

16. Koya, T.; Yanagisawa, R.; Higuchi, Y.; Sano, K.; Shimodaira, S. Interferon-α-Inducible Dendritic Cells Matured with OK-432 Exhibit TRAIL and Fas Ligand Pathway-Mediated Killer Activity. *Sci. Rep.* **2017**, *7*, 42145. [CrossRef]

17. Spadaro, F.; Lapenta, C.; Donati, S.; Abalsamo, L.; Barnaba, V.; Belardelli, F.; Santini, S.M.; Ferrantini, M. IFN-α Enhances Cross-Presentation in Human Dendritic Cells by Modulating Antigen Survival, Endocytic Routing, and Processing. *Blood* **2012**, *119*, 1407–1417. [CrossRef]

18. Papewalis, C.; Jacobs, B.; Wuttke, M.; Ullrich, E.; Baehring, T.; Fenk, R.; Willenberg, H.S.; Schinner, S.; Cohnen, M.; Seissler, J.; et al. IFN-Alpha Skews Monocytes into CD56+-Expressing Dendritic Cells with Potent Functional Activities In Vitro and In Vivo. *J. Immunol. Baltim.* **2008**, *180*, 1462–1470. [CrossRef]

19. Rozera, C.; Cappellini, G.A.; D'Agostino, G.; Santodonato, L.; Castiello, L.; Urbani, F.; Macchia, I.; Aricò, E.; Casorelli, I.; Sestili, P.; et al. Intratumoral Injection of IFN-Alpha Dendritic Cells after Dacarbazine Activates Anti-Tumor Immunity: Results from a Phase I Trial in Advanced Melanoma. *J. Transl. Med.* **2015**, *13*, 139. [CrossRef]

20. Cox, M.C.; Castiello, L.; Mattei, M.; Santodonato, L.; D'Agostino, G.; Muraro, E.; Martorelli, D.; Lapenta, C.; Di Napoli, A.; Di Landro, F.; et al. Clinical and Antitumor Immune Responses in Relapsed/Refractory Follicular Lymphoma Patients after Intranodal Injections of IFNα-Dendritic Cells and Rituximab: A Phase I Clinical Trial. *Clin. Cancer Res. Off. J. Am. Assoc. Cancer Res.* **2019**, *25*, 5231–5241. [CrossRef]

21. Li, C.Y.; Wu, X.Y.; Tong, J.B.; Yang, X.X.; Zhao, J.L.; Zheng, Q.F.; Zhao, G.B.; Ma, Z.J. Comparative Analysis of Human Mesenchymal Stem Cells from Bone Marrow and Adipose Tissue under Xeno-Free Conditions for Cell Therapy. *Stem Cell Res. Ther.* **2015**, *6*, 55. [CrossRef] [PubMed]

22. Von Bonin, M.; Stölzel, F.; Goedecke, A.; Richter, K.; Wuschek, N.; Hölig, K.; Platzbecker, U.; Illmer, T.; Schaich, M.; Schetelig, J.; et al. Treatment of Refractory Acute GVHD with Third-Party MSC Expanded in Platelet Lysate-Containing Medium. *Bone Marrow Transplant.* **2009**, *43*, 245–251. [CrossRef] [PubMed]

23. Siegel, G.; Fleck, E.; Elser, S.; Hermanutz-Klein, U.; Waidmann, M.; Northoff, H.; Seifried, E.; Schäfer, R. Manufacture of Endothelial Colony-Forming Progenitor Cells from Steady-State Peripheral Blood Leukapheresis Using Pooled Human Platelet Lysate. *Transfusion* **2018**, *58*, 1132–1142. [CrossRef] [PubMed]

24. Daniliuc, S.; Genser-Nir, M.; Miropolski, Y.; Sharovetsky, M.; Hazan Brill, R.H.; Fiorentini, D.; McNiece, I.; Kellner, J. Cell Therapy-Compliant Xeno-Free Culture System for Human Endothelial Cells. *Cytotherapy* **2018**, *20*, S86. [CrossRef]

25. Fekete, N.; Gadelorge, M.; Fürst, D.; Maurer, C.; Dausend, J.; Fleury-Cappellesso, S.; Mailänder, V.; Lotfi, R.; Ignatius, A.; Sensebé, L.; et al. Platelet Lysate from Whole Blood-Derived Pooled Platelet Concentrates and Apheresis-Derived Platelet Concentrates for the Isolation and Expansion of Human Bone Marrow Mesenchymal Stromal Cells: Production Process, Content and Identification of Active Components. *Cytotherapy* **2012**, *14*, 540–554. [CrossRef]

26. Švajger, U. Human Platelet Lysate Is a Successful Alternative Serum Supplement for Propagation of Monocyte-Derived Dendritic Cells. *Cytotherapy* **2017**, *19*, 486–499. [CrossRef]

27. Kral, J.B.; Schrottmaier, W.C.; Salzmann, M.; Assinger, A. Platelet Interaction with Innate Immune Cells. *Transfus. Med. Hemother.* **2016**, *43*, 78–88. [CrossRef]

28. Shimodaira, S.; Koya, T.; Higuchi, Y.; Okamoto, M.; Koido, S. Quality Verification of Dendritic Cell-Based Cancer Vaccine. *Pharm. Anal. Acta* **2015**, *7*. [CrossRef]

29. Korthals, M.; Safaian, N.; Kronenwett, R.; Maihöfer, D.; Schott, M.; Papewalis, C.; Diaz Blanco, E.; Winter, M.; Czibere, A.; Haas, R.; et al. Monocyte Derived Dendritic Cells Generated by IFN-α Acquire Mature Dendritic and Natural Killer Cell Properties as Shown by Gene Expression Analysis. *J. Transl. Med.* **2007**, *5*, 46. [CrossRef]

30. Tekkatte, C.; Gunasingh, G.; Cherian, K.; Sankaranarayanan, K. "Humanized" Stem Cell Culture Techniques: The Animal Serum Controversy. *Stem Cells Int.* **2011**, *2011*, 1–14. [CrossRef]

31. Presciutti, S.M.; Paglia, D.N.; Karukonda, T.; Soung, D.Y.; Guzzo, R.; Drissi, H.; Moss, I.L. PDGF-BB Inhibits Intervertebral Disc Cell Apoptosis in Vitro. *J. Orthop. Res.* **2014**, *32*, 1181–1188. [CrossRef] [PubMed]

32. Hsu, W.Y.; Chao, Y.W.; Tsai, Y.L.; Lien, C.C.; Chang, C.F.; Deng, M.C.; Ho, L.T.; Kwok, C.F.; Juan, C.C. Resistin Induces Monocyte–Endothelial Cell Adhesion by Increasing ICAM-1 and VCAM-1 Expression in Endothelial Cells via P38MAPK-Dependent Pathway. *J. Cell. Physiol.* **2011**, *226*, 2181–2188. [CrossRef] [PubMed]

33. Liu, X.; Wang, L.; Ma, C.; Wang, G.; Zhang, Y.; Sun, S. Exosomes Derived from Platelet-Rich Plasma Present a Novel Potential in Alleviating Knee Osteoarthritis by Promoting Proliferation and Inhibiting Apoptosis of Chondrocyte via Wnt/β-Catenin Signaling Pathway. *J. Orthop. Surg.* **2019**, *14*, 470. [CrossRef] [PubMed]

34. Dudek, A.M.; Martin, S.; Garg, A.D.; Agostinis, P. Immature, Semi-Mature, and Fully Mature Dendritic Cells: Toward a DC-Cancer Cells Interface That Augments Anticancer Immunity. *Front. Immunol.* **2013**, *4*, 438. [CrossRef]

35. Rutella, S.; Danese, S.; Leone, G. Tolerogenic Dendritic Cells: Cytokine Modulation Comes of Age. *Blood* **2006**, *108*, 1435–1440. [CrossRef]

36. Barratt-Boyes, S.M.; Zimmer, M.I.; Harshyne, L.A.; Meyer, E.M.; Watkins, S.C.; Capuano, S.; Murphey-Corb, M.; Falo, L.D.; Donnenberg, A.D. Maturation and Trafficking of Monocyte-Derived Dendritic Cells in Monkeys: Implications for Dendritic Cell-Based Vaccines. *J. Immunol.* **2000**, *164*, 2487–2495. [CrossRef]

37. Barratt-Boyes, S.M.; Watkins, S.C.; Finn, O.J. In Vivo Migration of Dendritic Cells Differentiated In Vitro: A Chimpanzee Model. *J. Immunol.* **1997**, *158*, 4543–4547.

38. Padovan, E.; Spagnoli, G.C.; Ferrantini, M.; Heberer, M. IFN-alpha2a Induces IP-10/CXCL10 and MIG/CXCL9 Production in Monocyte-Derived Dendritic Cells and Enhances Their Capacity to Attract and Stimulate CD8+ Effector T Cells. *J. Leukoc. Biol.* **2002**, *71*, 669–676. [CrossRef]

39. Muthuswamy, R.; Mueller-Berghaus, J.; Haberkorn, U.; Reinhart, T.A.; Schadendorf, D.; Kalinski, P. PGE2 Transiently Enhances DC Expression of CCR7 but Inhibits the Ability of DCs to Produce CCL19 and Attract Naive T Cells. *Blood* **2010**, *116*, 1454–1459. [CrossRef]

40. Butte, M.J.; Keir, M.E.; Phamduy, T.B.; Sharpe, A.H.; Freeman, G.J. Programmed Death-1 Ligand 1 Interacts Specifically with the B7-1 Costimulatory Molecule to Inhibit T Cell Responses. *Immunity* **2007**, *27*, 111–122. [CrossRef]

41. Peng, Q.; Qiu, X.; Zhang, Z.; Zhang, S.; Zhang, Y.; Liang, Y.; Guo, J.; Peng, H.; Chen, M.; Fu, Y.X.; et al. PD-L1 on Dendritic Cells Attenuates T Cell Activation and Regulates Response to Immune Checkpoint Blockade. *Nat. Commun.* **2020**, *11*, 4835. [CrossRef] [PubMed]

42. Francisco, L.M.; Salinas, V.H.; Brown, K.E.; Vanguri, V.K.; Freeman, G.J.; Kuchroo, V.K.; Sharpe, A.H. PD-L1 Regulates the Development, Maintenance, and Function of Induced Regulatory T Cells. *J. Exp. Med.* **2009**, *206*, 3015–3029. [CrossRef] [PubMed]

43. Han, P.; Hanlon, D.; Arshad, N.; Lee, J.S.; Tatsuno, K.; Robinson, E.; Filler, R.; Sobolev, O.; Cote, C.; Rivera-Molina, F.; et al. Platelet P-Selectin Initiates Cross-Presentation and Dendritic Cell Differentiation in Blood Monocytes. *Sci. Adv.* **2020**, *6*, eaaz1580. [CrossRef] [PubMed]

44. Collins, H.L.; Bancroft, G.J. Cytokine Enhancement of Complement-Dependent Phagocytosis by Macrophages: Synergy of Tumor Necrosis Factor-α and Granulocyte-Macrophage Colony-Stimulating Factor for Phagocytosis of Cryptococcus neoformans. *Eur. J. Immunol.* **1992**, *22*, 1447–1454. [CrossRef] [PubMed]

45. Dikic, I. Mechanisms Controlling EGF Receptor Endocytosis and Degradation. *Biochem. Soc. Trans.* **2003**, *31*, 1178–1181. [CrossRef]

46. Ming, J.E.; Steinman, R.M.; Granelli-Piperno, A. IL-6 Enhances the Generation of Cytolytic T Lymphocytes in the Allogeneic Mixed Leucocyte Reaction. *Clin. Exp. Immunol.* **1992**, *89*, 148–153. [CrossRef]

47. Mosser, D.M.; Zhang, X. Interleukin-10: New Perspectives on an Old Cytokine. *Immunol. Res.* **2008**, *226*, 205–218. [CrossRef]

48. Santin, A.D.; Hermonat, P.L.; Ravaggi, A.; Bellone, S.; Pecorelli, S.; Roman, J.J.; Parham, G.P.; Cannon, M.J. Interleukin-10 Increases Th1 Cytokine Production and Cytotoxic Potential in Human Papillomavirus-Specific CD8+ Cytotoxic T Lymphocytes. *J. Virol.* **2000**, *74*, 4729–4737. [CrossRef]

49. Fujii, S.; Shimizu, K.; Shimizu, T.; Lotze, M.T. Interleukin-10 Promotes the Maintenance of Antitumor CD8+ T-Cell Effector Function In Situ. *Blood* **2001**, *98*, 2143–2151. [CrossRef]

50. Scheurich, P.; Thoma, B.; Ucer, U.; Pfizenmaier, K. Immunoregulatory Activity of Recombinant Human Tumor Necrosis Factor (TNF)-Alpha: Induction of TNF Receptors on Human T Cells and TNF-Alpha-Mediated Enhancement of T Cell Responses. *J. Immunol. Baltim. MD* **1950**, *138*, 1786–1790, 1987.

51. Del Vecchio, M.D.; Bajetta, E.; Canova, S.; Lotze, M.T.; Wesa, A.; Parmiani, G.; Anichini, A. Interleukin-12: Biological Properties and Clinical Application. *Clin. Cancer Res.* **2007**, *13*, 4677–4685. [CrossRef] [PubMed]

52. Strobl, H.; Knapp, W. TGF-B1 Regulation of Dendritic Cells. *Microbes Infect.* **1999**, *1*, 1283–1290. [CrossRef]

53. Clausen, B.E.; Stoitzner, P. Functional Specialization of Skin Dendritic Cell Subsets in Regulating T Cell Responses. *Front. Immunol.* **2015**, *6*, 534. [CrossRef] [PubMed]

54. Klechevsky, E.; Morita, R.; Liu, M.; Cao, Y.; Coquery, S.; Thompson-Snipes, L.; Briere, F.; Chaussabel, D.; Zurawski, G.; Palucka, A.K.; et al. Functional Specializations of Human Epidermal Langerhans Cells and CD14+ Dermal Dendritic Cells. *Immunity* **2008**, *29*, 497–510. [CrossRef] [PubMed]